

AperTO - Archivio Istituzionale Open Access dell'Università di Torino

**Parallel dual secondary column-dual detection: A further way of enhancing the informative potential of two-dimensional comprehensive gas chromatography**

**This is the author's manuscript**

*Original Citation:*

*Availability:*

This version is available <http://hdl.handle.net/2318/148168> since 2016-12-01T13:10:54Z

*Published version:*

DOI:10.1016/j.chroma.2014.07.081

*Terms of use:*

Open Access

Anyone can freely access the full text of works made available as "Open Access". Works made available under a Creative Commons license can be used according to the terms and conditions of said license. Use of all other works requires consent of the right holder (author or publisher) if not exempted from copyright protection by the applicable law.

(Article begins on next page)



## UNIVERSITÀ DEGLI STUDI DI TORINO

This Accepted Author Manuscript (AAM) is copyrighted and published by Elsevier. It is posted here by agreement between Elsevier and the University of Turin. Changes resulting from the publishing process - such as editing, corrections, structural formatting, and other quality control mechanisms - may not be reflected in this version of the text. The definitive version of the text was subsequently published in [*Journal of Chromatography A*, Volume 1360, 19 September 2014, Pages 264–274. DOI: 10.1016/j.chroma.2014.07.081].

You may download, copy and otherwise use the AAM for non-commercial purposes provided that your license is limited by the following restrictions:

- (1) You may use this AAM for non-commercial purposes only under the terms of the CC-BY-NC-ND license.
- (2) The integrity of the work and identification of the author, copyright owner, and publisher must be preserved in any copy.
- (3) You must attribute this AAM in the following format: Creative Commons BY-NC-ND license (<http://creativecommons.org/licenses/by-nc-nd/4.0/deed.en>), [<http://dx.doi.org/10.1016/j.chroma.2014.07.081>]

**Parallel dual secondary column-dual detection:  
a further way of enhancing the informative potential of two-dimensional  
comprehensive gas chromatography**

Luca Nicolotti<sup>1</sup>, Chiara Cordero<sup>2\*</sup>, Davide Bressanello<sup>2</sup>, Cecilia Cagliero<sup>2</sup>, Erica Liberto<sup>2</sup>, Federico Magagna<sup>2</sup>,  
Patrizia Rubiolo<sup>2</sup>, Barbara Sgorbini<sup>2</sup> and Carlo Bicchi<sup>2</sup>

<sup>1</sup>Author's affiliation:

Faculty of Chemistry, Technical University of Munich; Lise-Meitner-Strasse 34, 85354 Freising, Germany

<sup>2</sup>Authors' affiliation:

Dipartimento di Scienza e Tecnologia del Farmaco, Università di Torino, Via Pietro Giuria 9, I-10125 Turin,  
Italy

\* Address for correspondence:

Dr. Chiara Cordero - Dipartimento di Scienza e Tecnologia del Farmaco, Università di Torino, Via Pietro  
Giuria 9, I-10125 Torino, Italy – e-mail: chiara.cordero@unito.it ; phone: +39 011 6707662; fax: +39 011  
2367662

24 **Abstract**

25 Comprehensive two-dimensional gas chromatography (GC×GC) coupled with Mass Spectrometry (MS) is  
26 one of today's most powerful analytical platforms for detailed analysis of medium-to-high complexity  
27 samples. The column set usually consists of a long, conventional-inner-diameter first dimension (<sup>1</sup>D)  
28 (typically 15-30 m long, 0.32-0.25 mm *d<sub>i</sub>*), and a short, narrow-bore second dimension (<sup>2</sup>D) column  
29 (typically 0.5-2 m, 0.1 mm *d<sub>i</sub>*) where separation is run in a few seconds. However, when thermal  
30 modulation is used, since the columns of a set are coupled in series, a flow mismatch occurs between the  
31 two dimensions, making it impossible to operate simultaneously at optimized flow conditions. Further,  
32 short narrow-bore capillaries can easily be overloaded, because of their lower loadability, limiting the  
33 effectiveness of <sup>2</sup>D separation.

34 In this study, improved gas linear velocities in both chromatographic dimensions were achieved by coupling  
35 the <sup>1</sup>D column with two parallel <sup>2</sup>D columns, having identical inner diameter, stationary phase chemistry,  
36 and film thickness. In turn, these were connected to two detectors: a fast quadrupole Mass Spectrometer  
37 (MS) and a Flame Ionization Detector (FID). Different configurations were tested and performances  
38 compared to a conventional set-up; experimental results on two model mixtures (*n*-alkanes and fourteen  
39 medium-to-high polarity volatiles of interest in the flavor and fragrance field) and on the essential oil of  
40 *Artemisia umbelliformis* Lam., show the system provides consistent results, in terms of analyte  
41 identification (reliability of spectra and MS matching) and quantitation, also affording an internal cross-  
42 validation of quantitation accuracy.

43

44

45 **Key-words:**

46 Two-dimensional comprehensive gas chromatography-mass spectrometry; parallel dual secondary column-  
47 dual detection; dual <sup>2</sup>D pattern alignment, outlet pressure correction, second dimension linear velocity  
48 optimization, essential oil analysis

49

## 50 1. Introduction

51 Comprehensive two-dimensional gas chromatography (GC×GC) coupled with Mass Spectrometry  
52 (MS) is one of the most powerful analytical platforms now available for the detailed analysis (identification  
53 and quantitation) of medium-to-high complexity samples. Compared to one-dimensional systems, it offers  
54 remarkable separation power and unmatched peak capacity [1,2]; the possibility of applying different  
55 separation mechanisms in the two chromatographic dimensions produces rationalized 2D patterns, suitable  
56 as sample fingerprints for classification and identification purposes [3].

57 The most common GC×GC column sets consist of a long, conventional-inner-diameter first dimension (<sup>1</sup>D)  
58 (typically 15–30 m long and 0.32–0.25 mm  $d_c$ ), and a short, narrow-bore second dimension (<sup>2</sup>D) column  
59 (typically 0.5–2 m 0.1 mm  $d_c$ ). Thanks to the short narrow-bore <sup>2</sup>D column, the separation is run in a few  
60 seconds, both minimizing wrap-around phenomena and contributing to the high efficiency of the system.  
61 However, when thermal modulation is used, since the columns of a set are coupled in series, a flow  
62 mismatch occurs between the two dimensions; this makes it impossible to operate simultaneously at  
63 optimized flow conditions. In addition, short narrow-bore capillaries can easily overload, because of their  
64 lower loadability, limiting <sup>2</sup>D separation effectiveness [4,5]. The configuration and optimization of a GC×GC  
65 set-up is thus a crucial, but also a complex step, since separation in the two dimensions is differently  
66 influenced in the two separation dimensions by carrier gas flow, temperature, and modulation period. With  
67 regard to the flow regime, in their earlier publications Phillips *et al* [6,7] indicated a possible way of  
68 optimizing carrier gas flow by splitting part of the flow from <sup>1</sup>D to waste, prior to modulation. They adopted  
69 a Tee union to connect the two analytical columns, and a short capillary segment enabling the diversion of  
70 about 30% of the primary column flow to waste, thus applying flows closer to the optimal in both  
71 dimensions, and reducing overloading of the <sup>2</sup>D.

72 In 2007, Tranchida *et al.* [8] included a flow splitter in a classical GC×GC-FID system. The method, called  
73 “split-flow” comprehensive 2D-GC, consisted of a <sup>1</sup>D apolar 30 m × 0.25 mm  $d_c$  column, connected to a 1 m  
74 × 0.10 mm  $d_c$  polar <sup>2</sup>D and to an uncoated capillary of 30 cm × 0.10 mm  $d_c$ , using a Y press fit. The carrier  
75 gas (hydrogen) linear velocities were regulated thanks to a manually-operated split valve, connected to the  
76 uncoated capillary. Experimental results on Fatty Acids Methyl Esters (FAMES) from a cod oil sample  
77 showed that, with a 35:65 (FID) split-flow ratio and 146.3 kPa head pressure, gas velocities close to optimal  
78 could be obtained (i.e., about 35 and 213 cm/sec in the <sup>1</sup>D and <sup>2</sup>D respectively) with a positive effect on  
79 separation efficiency and resolution (+50% for a selected critical pair) while maintaining structured  
80 chromatograms.

81 Other straightforward solutions have been proposed to overcome this critical issue, which is known as flow-  
82 mismatch in the two dimensions. In stop-flow GC×GC [9–11] the <sup>1</sup>D flow is periodically halted and during  
83 each pause the <sup>2</sup>D separation continues, by delivering carrier gas via an auxiliary pressure controller. This

latter set-up enables column flow to be independently regulated, thus optimizing the separation in both dimensions.

Another possibility is to adopt wider <sup>2</sup>D capillaries [12,13]; if columns of a set have the same inner diameter, flow conditions closer to optimal can be applied in both dimensions, improving the exploitation of the <sup>2</sup>D stationary phase selectivity, even at higher temperature rates, and at the same time increasing <sup>2</sup>D column loadability [12]. Experimental results on medium-complexity samples of interest in the flavor and fragrance field, with homologous  $d_c$  column sets, show that the mean loss of peak capacity (by a factor of 3; System Separation Measure -  $S_{GC \times GC}$ ) is partially or fully compensated, thanks to better exploitation of <sup>2</sup>D stationary phase selectivity. At the same time, reliable quali-quantitative results are achieved, by complying with the minimal modulation requirements (Modulation Ratio criterion -  $M_R$ ) [13]. More recently, Peroni *et al.* evaluated two alternative solutions: (a) the use of monolithic <sup>2</sup>D columns [14], and (b) multiple capillary columns in parallel as <sup>2</sup>D [15]. With monoliths, efficiency and column flow can be optimized independently, but at the cost of poor separation efficiency. However, multi-<sup>2</sup>D columns appear to be a good alternative; the carrier gas flow is divided over multiple-parallel <sup>2</sup>D flow paths, enabling both dimensions to be fully exploited at the same time. Unfortunately, as the authors themselves state, coupling the <sup>1</sup>D to the multi-<sup>2</sup>D is, in practice, rather a complex procedure, limiting the feasibility of such set-ups in routine use.

As discussed by Peroni and Janssen [16], the optimum linear velocities in both dimensions are reduced when the second dimension operates at high outlet pressure. The proposed set-up includes a restrictor at the outlet of the <sup>2</sup>D, prepared by melting the end of the column with a high-temperature hydrogen flame (1800°C) until closure, and then partially re-opening it, by grinding it with sandpaper, to obtain the desired flow. The elevated outlet pressure conditions resulted in flatter *Van Deemter* curves at higher velocities, causing a slower loss of efficiency at higher inlet pressures. Experimental results indicated that this system configuration is characterized by a slightly improved resolution for a given column set, compared to conventional pressure drops, but that the analysis time is longer.

In the present study, improved gas linear velocities in both chromatographic dimensions were achieved by coupling the <sup>1</sup>D column with two parallel <sup>2</sup>D columns having identical inner diameter, stationary phase chemistry, and film thickness, in turn connected to two detectors: a fast quadrupole Mass Spectrometer (MS), and a Flame Ionization Detector (FID). The system was equipped with a loop-type thermal modulator; cryotrapping and refocusing were set at the head of the <sup>2</sup>D capillaries to narrow bands entering the <sup>2</sup>D [17]. Three different column set-up were tested: the first, *Set-up I*, included a primary column connected with two parallel <sup>2</sup>Ds of different lengths (1.6 m x 0.1 mm  $d_c$  to MS and 1.4 m x 0.1 mm  $d_c$  to FID) but operating at an almost equal nominal flow (comparable hold-up times) although subjected to different outlet pressures. The second system configuration, *Set-up II*, included two identical <sup>2</sup>D columns (1.4 m x 0.1 mm  $d_c$ ) and an auxiliary pressure controller to deliver a supplementary flow of carrier gas at the outlet of the <sup>2</sup>D connected to the MS detector. The latter was inspired by the system proposed by Shellie *et al.* [18],

119 in which GC×GC-FID and GC×GC-TOF-MS chromatograms were successfully matched, obtaining almost  
120 identical 2D patterns thanks to the adjustment of inner and outlet pressures. Lastly a conventional set-up  
121 was taken as a reference, i.e. *Set-up III* consisted of a single <sup>2</sup>D column (total length including modulation  
122 loop: 1.4 m x 0.1 mm *d<sub>i</sub>*) connected to two parallel detectors, via splitting capillaries.

123 The performance of each *Set-up* are evaluated by analyzing two model mixtures (n-alkanes (HydStd1) and  
124 14 medium-to-high polarity volatiles in the flavor and fragrance field (FFStd2)), and the *Artemisia*  
125 *umbelliformis* Lam. essential oil. The potentials and limits of each set-up are also discussed in terms of  
126 separation performances and in view of the practical information that can be derived from each single  
127 analytical run.

128

## 129 **2. Experimental**

### 130 **2.1 Samples and solvents**

131 Pure standards of *n*-alkanes (from *n*-C9 to *n*-C25) for system evaluation, flow/pressure optimization and  
132 Linear Retention Indices (*I<sub>T</sub>*) determination were from Sigma-Aldrich (Milan, Italy).

133 Pure standards of α-pinene, benzaldehyde, benzyl alcohol, α-thujone, camphor, carvone, cinnamyl alcohol,  
134 geranyl acetate, vanillin, coumarin, isoeugenol, isoeugenyl acetate, benzyl benzoate, and sclareol, were  
135 from Sigma-Aldrich (Milan, Italy). The two model mixtures (i.e., HydStd1 and FFStd2) for system evaluation  
136 were prepared by mixing single component Standard Mother Solutions, at 10 g/L in dichloromethane, and  
137 adjusting the final volume up to 100 mg/L. Solvents were all HPLC-grade, from Riedel-de Haen (Seelze,  
138 Germany).

139 *Artemisia umbelliformis* Lam. essential oil (EO) was prepared following the method of the European  
140 Pharmacopoeia [19]. Ten grams of dried aerial parts from experimental cultivations run in different alpine  
141 valleys were suspended in 250 mL of water in a 500 mL flask for 1 h, and then submitted to hydrodistillation  
142 in a Clevenger micro-apparatus for 2 hours [20]. The resulting EO was left to stabilize for 1 h, then  
143 recovered and analyzed directly.

144

### 145 **2.2 GC×GC instrument set-up**

146 GC×GC analyses were run with a system configured as follows: a HT280T multipurpose sampler (HTA,  
147 Brescia, Italy) was integrated with an Agilent 6890 GC unit coupled to an Agilent 5975C MS detector  
148 (Agilent, Little Falls, DE, USA) operating in EI mode at 70 eV. The GC transfer line was set at 280°C. A  
149 *Standard Tune* was used and the scan range was set to *m/z* 40-300 with a scanning rate of 12,500 amu/s to  
150 obtain a spectra generation frequency of 28 Hz. The Flame Ionization Detector (FID) conditions were: base  
151 temperature 280°C, H<sub>2</sub> flow 40 mL/min; air flow 240 mL/min; make-up (N<sub>2</sub>) 450 mL/min; sampling  
152 frequency 150 Hz.

153 Injections of the essential oil, and of the two model mixtures, as well as those for  $I_s^T$  determination  
154 samples, were by HT280T sampler (HTA, Brescia, Italy) under the following conditions: split/splitless  
155 injector, split mode, split ratio 1/50, injector temperature 280°C, injection volume 0.1 µL of undiluted  
156 essential oil and 1µL of the *n*-HydStd1 and FFSTd2 model mixtures at 100 mg/L. The oven temperature was  
157 programmed as follows: 50°C (1 min) to 270°C at 3.0°C/min and to 290°C at 10°C/min (10 min).  
158 Flow/pressure optimization was checked on a standard solution of tridecane, tetradecane and pentadecane  
159 (n-C13 to n-C15) at 100 mg/L analyzed in isothermal conditions at 150°C. Head-pressure values are  
160 reported in **Table 1**.

161

## 162 **2.3 Thermal modulator parameters**

163 The system was equipped with a two-stage KT 2004 loop thermal modulator (Zoex Corporation, Houston,  
164 TX) cooled with liquid nitrogen controlled by Optimode™ V.2 (SRA Instruments, Cernusco sul Naviglio, MI,  
165 Italy). Hot jet pulse time was set at 250 ms, modulation time was 5 s and cold-jet total flow progressively  
166 reduced with a linear function, from 40% of Mass Flow Controller (MFC) at initial conditions, to 5% at the  
167 end of the run. Loop dimensions were chosen on the basis of the expected carrier linear velocities, to  
168 ascertain that at least two stage-band-focusing releases were performed for each modulation. Thus, for all  
169 *Set-ups*, the first 0.6 m of the <sup>2</sup>Ds war wrapped in the metal slit of the modulator.

170

## 171 **2.4 Column connections and auxiliary control module**

172 Connections between the primary and the two secondary columns (*Set-ups I* and *II*), and between the  
173 secondary column and the deactivated capillaries for FID/MS effluent splitting (*Set-up III*) was via a SilFlow™  
174 GC 3 Port Splitter (SGE Ringwood, Victoria, Australia). The auxiliary pressure controller consisted of a one  
175 channel Pneumatics Control Module (G2317A) connected to a Quick Swap unit (G3185, Agilent, Little Falls,  
176 DE, USA) with a restrictor capillary of 0.17 m x 0.1 mm d<sub>c</sub>. A diagram of the system configuration is provided  
177 as Supplementary File (Supplementary Figure 1 - SF1).

178 Column set configurations are listed in **Table 1**, together with carrier gas head pressures and calculated  
179 linear velocities [18,21].

180

## 181 **2.5 Data acquisition and 2D plot elaboration**

182 Data were acquired by Agilent MSD ChemStation ver D.02.00.275 and processed using GC Image GC×GC  
183 Software version 2.1b1 (GC Image, LLC Lincoln NE, USA).

184

## 185 **3. Results and discussion**

### 186 **3.1 Some theoretical aspects**



187 Conventional GC×GC configurations with thermal modulators imply that the two columns of the set are  
 188 connected in series and the volumetric flow rates and linear velocities in the two capillaries are correctly  
 189 calculated; the pressure drop across the total length must also be estimated [8,18] ,.

190 The outlet column volumetric flow ( $F_{o(c)}$ ) can be derived by the Poiseuille equation (Eq. 1)

191

$$192 \quad F_{o(c)} = \frac{60\pi r^4}{16\eta L} \frac{(p_i^2 - p_o^2)}{p_o} \frac{T_{ref}}{T} \quad \text{Equation 1}$$

193

194 where  $r$  is the column radius,  $\eta$  the dynamic viscosity of the carrier gas at a given temperature,  $L$  is the  
 195 column length,  $p_i$  and  $p_o$  are the absolute inlet and outlet pressures, and  $T_{ref}$  is the reference temperature  
 196 (typically 298K) and  $T$  is the absolute operative temperature.

197 The pressure at any point ( $z$ ) along the column can be calculated according to Equation 2:

198

$$199 \quad p_z = \sqrt{p^2 - \left(\frac{z}{L}\right) (p^2 - 1)} \quad \text{Equation 2}$$

200

201 The linear velocity at the column outlet ( $u_o$ ) is:

202

$$203 \quad u_o = \left( \frac{r^4 (p_i^2 - p_o^2)}{16\eta L p_o} \right) \quad \text{Equation 3}$$

204

205 where  $r$  is the column radius,  $\eta$  the dynamic viscosity of the carrier gas at the operating temperature,  $L$  is  
 206 the column length,  $p_i$  and  $p_o$  are the absolute inlet and outlet pressures. The average velocity is proportional  
 207 to the outlet velocity corrected by the compression factor  $j$ :

$$208 \quad \bar{u} = u_o \cdot j \quad \text{Equation 4}$$

209 where

$$210 \quad j = \frac{3 (p^2 - 1)}{2 (p^3 - 1)} \quad \text{Equation 5}$$

211

212 The average linear velocity along each separation dimension can be estimated by combining the above  
 213 functions. **Table 1** reports average linear velocities, calculated at 333 K (60°C), together with inlet pressure  
 214 ( $p_i$ ), midpoint pressure ( $p_2$ ) at the connection between primary and secondary column(s) in kPa (over  
 215 pressure) and hold-up times (s). In the case of *Set-up II*, the data do not include the adjustment of outlet  
 216 pressure by the auxiliary flow controller.

217

### 218 **3.2 Parallel dual secondary columns operating at different outlet pressures (GC×2GC-MS/FID)**

219 The first part of this study was carried out on dual parallel columns of identical inner diameter (i.e., 0.10  
220 mm  $d_c$ ) but of an almost equivalent length in terms of flow resistance. *Set-up I* was inspired by the “split-  
221 flow” configuration proposed by Tranchida *et al.* [17], with the sole difference that the outlet of the split  
222 capillary (an OV1701 capillary column with 0.10  $\mu\text{m}$   $d_f$ ) was connected to a FID detector (atmospheric  
223 pressure). Compared to a conventional configuration (*Set-up III*), where one of the two dimensions has to  
224 operate very far from its optimum performance, whatever the head pressure, in *Set-up I* close-to-optimal  
225 linear velocities in both chromatographic dimensions are applied, i.e.  $^1\text{D}$  at about 34 cm/s and the  $^2\text{Ds}$  at  
226 about 180 cm/s (see **Table 1**).

227 Differences in secondary column length were expected to condition the separation in terms of absolute  
228 retention and peak-widths. However, the resulting 2D patterns were expected to be consistent, although  
229 not identical. According to Schutjes *et al.* [21], who rearranged the *Golay* plate height equation in terms of  
230 dimensionless parameters (i.e.,  $\xi = H/H_{\min}$  and  $v = \bar{u}/\bar{u}_{\text{opt}}$ ), operating at  $p_i/p_o \gg 1$  (i.e., vacuum outlet), the  
231 maximum efficiency is reached for a close interval of average linear velocities around  $\bar{u}_{\text{opt}}$ . Conversely, when  
232  $p_i/p_o$  approaches unity (i.e. at ambient pressure), the experimental curve of  $H/H_{\min}$  as a function of  $\bar{u}/\bar{u}_{\text{opt}}$  is  
233 flatter, and enables a better separation efficiency. With *Set-up I* lower efficiencies were expected for the  
234 MS branch [21] also in consequence of the longitudinal diffusion effect.

235 The experimental results confirmed these hypotheses: **Figure 1** shows the raw chromatogram overlaid with  
236 2D plots of linear hydrocarbons from C13 to C15 analyzed in isothermal conditions (i.e., 150°C) at 296 kPa  
237 head-pressure with *Set-ups I* and *II*. System hold-up times, measured experimentally with methane  
238 injections at 80% of MFC cold jet regulation, were 1.905 min and 0.86 s in the  $^1\text{D}$  and  $^2\text{D}$  respectively, in fair  
239 accordance with the expected values. Alkanes showed an absolute retention time shift (MS vs. FID) of -0.18  
240 s for n-C13 and of -0.36 s for n-C15. Although minimized by the lower retention in the second dimension  
241 due to the temperature of the isothermal analysis, a much larger mismatch was expected for temperature  
242 programmed conditions and strongly retained analytes.

243 **Figure 2** reports 2D plots (**Fig. 2a** full scan MS and **Fig. 2b** FID plots) of *Artemisia umbelliformis* essential oil,  
244 analyzed with *Set-up I*. The consistency of the 2D patterns of the two detectors is evident; the structured  
245 patterns of mono-terpenoid (*m*) and sesqui-terpenoid (*s*) hydrocarbons are clearly organized, and  
246 separated from the oxygenated derivatives (*mox* and *sox*) and from other secondary metabolites (mono  
247 terpenoid esters - *mest*). More polar compounds (carbonyl derivatives, alcohols and esters) having greater  
248 affinity for the second dimension stationary phase were more strongly retained along the  $^2\text{D}$  branch  
249 towards MS (higher retention factors - *k*).

250 The magnitude of the retention time shift is better illustrated in **Figures 3a** and **3b**, which show  $^2\text{D}$  retention  
251 time absolute differences (FID vs. MS) for: (**3a**) *n-alkane* hydrocarbons from *n*-C9 to *n*-C25 and (**3b**)  
252 fourteen volatiles of interest in flavor and fragrance applications. For the *n*-alkanes, where retention in the  
253  $^2\text{D}$  is negligible, absolute differences in retention times in no case exceeded (-)0.15 s (i.e., 3% as relative %

254 difference over 5 seconds of  $^2D$  separation time); conversely,  $^2D$  retention shifts for more polar compounds  
255 (**Fig. 3b**) were larger with differences between MS and FID patterns ranging from the (-)0.12 s of  $\alpha$ -pinene  
256 to the (-) 0.68 s of vanillin (i.e., 2.38 and 13.6 % of relative difference). Marked differences were recorded  
257 for the more polar analytes (benzyl alcohol, cinnamyl alcohol, vanillin, isoeugenol and isoeugenyl acetate)  
258 that suffered from the wrap-around phenomenon.

259

### 260 **3.3 Parallel dual secondary columns operating at equivalent (atmospheric) outlet pressures (GC $\times$ 2GC-MS/FID)**

261

262 The study continued, adopting two secondary columns with the same number of theoretical plates and the  
263 same equivalent lengths, in terms of flow resistance; in addition a correction of the pressure drop across  
264 dimensions was operated by an auxiliary flow/pressure controller (EPC) connected to a microfluidic device  
265 installed between the outlet of the  $^2D_{MS}$  column and the MS transfer line (restrictor) [18].

266 In *Set-up II*, the two  $^2D$  columns were both 1.4 meters long (0.6 meters at the head of each column were  
267 wrapped to form the modulation loop) thus leaving available 0.8 meters of each column for separation. At  
268 the end of the  $^2D$  to MS, 0.17 m x 0.1 mm  $d_c$  of deactivated silica capillary (restrictor) was used to  
269 compensate for differences in flow resistance (**Table 1: Set-up II - auxiliary off conditions**). Additional  
270 helium flow was delivered by setting the auxiliary EPC at 40 kPa (5.7 psi relative) to adjust the outlet  
271 pressure towards MS. The compensation was minimal, because of the low resistance of the two parallel  
272  $^2Ds$ .

273 The outlet pressure correctness was verified by isothermal analysis (i.e., 150°C) of linear hydrocarbons from  
274 C13 to C15 at 296 kPa head-pressure; **Figure 1b** shows the raw chromatograms overlaid with the FID  $^2D$  plot  
275 resulting from an outlet pressure correction towards MS of 40 kPa. System hold-up times were 1.91 min  
276 and 0.88 s in the  $^1D$  and  $^2D$  respectively. Alkanes did not show any retention time shift. Experiments  
277 without outlet pressure correction were also run with test mixtures and under programmed temperature  
278 conditions; the relative difference between  $^2D$  retention times was on average 0.6 % for *n*-alkanes and 5.65  
279 % for the FFStd2 model mixture. Figures **3c** and **3d** show absolute differences in time values in detail. Again,  
280 wrapped-around analytes showed higher discrepancies between  $^2D$  elution times, due to accumulation of  
281 the delay error across subsequent modulations. However, with pressure compensation, the retention shift  
282 in no case exceeded 1.1 % for linear hydrocarbons and 4% (cinnamyl alcohol) for the FFStd2 model mixture  
283 components. These values are in agreement with those reported by Shellie *et al.* [18], although most of the  
284 analytes investigated in that study had lower retention in both dimensions.

285 **Figures 2c** and **2d** show the 2D plots (**Fig. 2c** full scan MS and **Fig. 2d** FID plot) of *Artemisia umbelliformis*  
286 essential oil, analyzed with *Set-up II* with auxiliary outlet compensation. As is clear, the 2D patterns are in  
287 this setup highly consistent, the structure is maintained, and the chromatographic space properly occupied.  
288 Experiments run without any outlet pressure correction (data not shown) produced 2D patterns with very

few differences from those shown, and this approach would be a good alternative when an additional EPC is not available, or turbo pumping systems do not tolerate high outlet flows. In such cases, adaptive algorithms (called *transforms*) for pattern recognition, like those used for template matching procedures [23] in targeted and untargeted data elaboration, can successfully compensate for <sup>2</sup>D retention times shifts, and consistently transfer identification from MS to FID.

### 3.4 Single secondary column with dual parallel detection (GC×GC-MS/FID)

To evaluate the practical advantages that can be obtained by operating at near-optimal linear velocities, with two parallel columns and two detection systems, an additional setup (*Set-up III*) consisting of a single <sup>2</sup>D column (1.4 m x 0.1 mm *d<sub>c</sub>*) connected to two parallel detectors was tested. Pressure/flow conditions adopted were a compromise between optimal conditions in both dimensions, and were allowed to run at 23 cm/s and 240 cm/s in the <sup>1</sup>D and in the <sup>2</sup>D, respectively. As expected, with *Set-up III* <sup>1</sup>D retention times slightly increased, reflecting the higher elution temperatures that resulted, while those in the <sup>2</sup>D decreased, due to the consequent loss of retention. **Figures 4a, 4b and 4d** show differences in retention times from *Set-up I* to *Set-up III*.

For *Artemisia umbelliformis* essential oil, although the separation structure was maintained, the overall resolution was lower. **Figures 2e and 2f** show the 2D patterns resulting from *Set-up III*. In this case, a concurrent reduction of the temperature rate and of the modulation period might be expected to produce better results, although analysis time is longer.

### 3.5 Practical advantages of the optimized GC×2GC-MS/FID platform

Some aspects deserve a brief discussion, to outline the practical advantages on real-world samples deriving from a GC×2GC-MS/FID platform, in terms of both dual <sup>2</sup>D column and dual detection. *Artemisia umbelliformis* essential oil was selected as a case study, since its detailed quantitative profiling is interesting for botanical classification, as well as in the light of quality aspects relating to its use to prepare a highly-prized Alpine liqueur, called “genepi”, characterized by a bitter taste and a distinctive aroma [24]. These sensory properties can be ascribed to terpenoids, in particular to α- and β-thujones, the main components of the volatile fraction for the aroma profile, and to sesquiterpene lactones with a *cis*-eudesmanolide skeleton (5-desoxy-5-hydroperoxy-5-epitelekin; 5-desoxy-5-hydroperoxytelekin and umbellifolide) for its bitterness [25]. The debate on the toxicity of thujones is still open [26], and European Union legislation has fixed a limit of 35 mg/kg on the total amount of these compounds in alcoholic beverages [27]. Thujone-free chemotypes of *A. umbelliformis* have been selectively bred to overcome this issue, and diagnostic fingerprints have been defined by combining biomolecular characterization with chemical profiling of informative secondary metabolites [25]. In any case, a detailed profiling of the volatile fraction is necessary to assess both sensory quality and safety of the aerial parts that are used to prepare the liqueur.

324 The first aspect to be considered is the separation power of GC×2GC-MS/FID. Resolution reflects the  
325 adequacy of the separation conditions adopted for a given group of target analytes, and becomes  
326 fundamental for samples where several informative peaks in variable abundances elute in a given region of  
327 the chromatographic space. Extra-chromatographic phenomena, e.g. column overloading, may in these  
328 cases condition correct separation, i.e. identification/quantitation. For example, when <sup>2</sup>D overloading  
329 occurs, minor peaks eluting in the proximity of highly abundant components, with large peak-width, may be  
330 lost, together with the information they carry. The <sup>2</sup>D dual column doubles the <sup>2</sup>D loadability, thus limiting  
331 <sup>2</sup>D overloading and loss of significant minor peaks due to this phenomenon. At the same time, the higher  
332 efficiency due to the average linear velocity closer to the optimal value, and the enhanced <sup>2</sup>D stationary  
333 phase selectivity, increase the system orthogonality, improving occupation of the chromatographic plane.  
334 For instance, the calculated α-thujone half-height peak width in the FFStd2 model mixture at 100 mg/L, was  
335 120 ms (see **Table 2**). In *A. umbelliformis* essential oil, α- and β-thujones are the two most abundant peaks,  
336 each with a peak width of 480 ms, that dramatically overloads the <sup>2</sup>D; in *Set-up III*, where the second  
337 dimension loadability is halved compared to *Set-up II*, they coelute in <sup>1</sup>D-GC with two minor components,  
338 i.e. nonanal and 2-methylbutyl isovalerate. Apparent resolution values (*R*) estimated on the raw  
339 chromatogram, and referred to the most abundant modulation for all compounds, were 1.93 for the 2-  
340 methylbutyl isovalerate/α-thujone pair with *Set-up II*, and 1.53 with *Set-up III*, while for the nonanal/α-  
341 thujone pair they were 1.28 for *Set-up II*, but coeluted in *Set-up III* (**Figure 5**).

342 A second practical aspect to consider for in attempting an overall evaluation of the potential of a GC×2GC-  
343 MS/FID system concerns quantitation reliability: this exploits the synergisms of dual detection operating by  
344 different principles. MS is known to provide a fundamental contribution to unequivocal analyte  
345 identification, while FID offers a wide dynamic range of linearity and a very high frequency of acquisition,  
346 thereby improving the accuracy of 2D peak (areas) volumes. Moreover, the correct alignment of the two  
347 patterns obtained with both *Setup II* and *Setup III* enables one to consider the data set from the two  
348 detectors as a single integrated system, thus cross-validating the results. These considerations are  
349 confirmed by experimental data on the FFStd2 mixture. **Table 2** shows <sup>1</sup>D and <sup>2</sup>D retention times and their  
350 absolute errors (<sup>2</sup>D Error in seconds), Normalized 2D Volumes for MS (TIC current) and FID signals  
351 (normalization was done on geranyl acetate), half-height peak-width (50% peak width (ms)) and the  
352 number of points per peak (MS operated at 28 Hz and FID at 150 Hz) for the analytes of FFStd2 mixture  
353 with *Set-up II* and *Set-up III*.

354 These results demonstrate that the chromatographic efficiency (expressed as half-height peak-width) is  
355 comparable for the two setups. It has to be stressed that *Set-up III* had to operate at <sup>2</sup>D flow conditions  
356 close to those adopted for the two-parallel-column system; if higher head-pressures had been applied,  
357 peak-widths would have been narrower. The number of points-per-peak was, in consequence, similar for

358 *Setup II* and *Setup III* for each detector, while mass quantitative descriptors (Normalized 2D Volumes) from  
359 the two detectors were consistent.

360 However, the potential of dual detection can concretely be perceived with real-world samples (e.g. *A.*  
361 *umbelliformis* essential oil). In these applications, the consistency of acquired MS spectra is fundamental  
362 since identification is mainly based on commercial spectral libraries. **Table 3** reports the <sup>1</sup>D Linear Retention  
363 Indices (experimental and reference values [28]), the MS match factors resulting from the NIST Identity  
364 Spectrum Search algorithm (NIST MS Search 2.0 ver. d) on spectra collected in commercial databases,  
365 and/or on spectra obtained by analyzing reference compounds, and the Signal-to-Noise (Peak-to-Peak S/N  
366 as calculated by the Agilent algorithm - SNR) estimated on the highest modulation of each 2D peak of the  
367 components characterizing *A. umbelliformis* essential oil.

368 For the selected analytes, the quality of the spectral match, as well as the S/N values were comparable  
369 between *Set-up II* and *III*. Higher S/N values would be expected for a conventional configuration, because of  
370 the sharper peaks generated at faster flow rates. Moreover, within the experimental conditions applied  
371 here, the <sup>2</sup>D peak widths generated were comparable (**Table 2**) and in accordance with the results recently  
372 obtained by Tranchida *et al.* [29].

373 Data reported in **Table 3** also show that the GC×2GC-MS/FID platform provides enhanced information,  
374 because the concurrent presence of two detectors not only provides contemporary analyte identification  
375 and quantitation, but also offers internal cross-validation of results. It is also important to note that the  
376 international guidelines for quantitative gas chromatography of volatile flavoring substances and essential  
377 oils [30-32] indicate Relative Response Factors (*RRF*) (i.e. external standard calibration with internal  
378 standard normalization) as the most suitable approach to obtain consistent quantitative data in these  
379 matrices, in particular with MS detection. However, for complex samples consisting of hundreds of  
380 potentially informative peaks, a full quantitative assessment by *RRFs* cannot be applied in practice. The  
381 internal normalization approach performed on the FID signal, also known as analyte percent normalization  
382 [31], is therefore accepted. In this case, the composition error is minimized by an appropriate selection of  
383 internal standard(s) and FID response factors [33-35] making true quantitation by *RRF* necessary only for  
384 those compounds that are limited by law (e.g.  $\alpha$ - and  $\beta$ -thujone). FID also opens the possibility of applying  
385 the approach introduced by de Saint Laumer *et al.* [36] where analytes' *RRFs* on FID signal are estimated on  
386 the basis of combustion enthalpies. With this approach, target analytes can be quantified through  
387 estimated *RRFs*, with accuracy errors limited to a few % points even without external standard calibration.  
388 Parallel dual detection thus seems to be very promising for reliable and simple qualitative component  
389 identification, and to quantitate markers of complex samples of natural origin.

390

#### 391 **4. Conclusions**

392 The advantages of using a dual-secondary-column dual-detection system in an integrated platform for  
393 GC×GC have been discussed, and some practical aspects concerning the tuning of experimental conditions  
394 to obtain consistent separation patterns from both dimensions have been addressed. These systems can  
395 operate at close-to-optimal <sup>2</sup>D linear velocities, and double the secondary column loading capacity, with  
396 positive effects on overall system orthogonality and resolution.

397 Experimental data also indicate that the GC×2GC-MS/FID system provides consistent results, both in terms  
398 of analyte identification (reliability of spectra and MS matching) and quantitation, also affording internal  
399 cross-validation of quantitation accuracy.

400 The choice of different setups, in terms of <sup>2</sup>D column dimensions and flow conditions, should take into  
401 consideration some critical aspects, including the auxiliary flow correction, which should be compatible  
402 with the turbo pumping capacity and the required sensitivity. The outlet pressure correction adopted in the  
403 present study was minimal, and compatible with both system-limiting factors.

404 These data open the way to investigating further applications, where system orthogonality and loading  
405 capacity are key-factors for successful separations.

406

#### 407 **Acknowledgements**

408 This study was supported by Ricerca Finanziata da Università - Fondo per la Ricerca Locale (Ex 60%) Anno  
409 2013.

410

411  
412  
413  
414  
415  
416  
417  
418  
419  
420  
421  
422  
423  
424  
425  
426  
427  
428  
429  
430  
431  
432  
433  
434  
435  
436  
437  
438  
439  
440  
441  
442  
443  
444  
445

**References**

1. M. Adahchour, J. Beens, R.J.J. Vreuls, U.A.Th. Brinkman, Recent developments in comprehensive two-dimensional gas chromatography (GC × GC): I. Introduction and instrumental set-up, Trends Anal. Chem. 25 (2006) 438-454.
2. H.J. Cortes, B. Winniford, J. Luong, M. Pursch, Comprehensive two dimensional gas chromatography review, J. Sep. Sci. 32 (2009) 883-904.
3. C. Cordero, E. Liberto, C. Bicchi, P. Rubiolo, P. Schieberle, S.E. Reichenbach, Q. Tao, Profiling food volatiles by comprehensive two-dimensional gas chromatography coupled with mass spectrometry: Advanced fingerprinting approaches for comparative analysis of the volatile fraction of roasted hazelnuts (*Corylus avellana* L.) from different origins, J. Chromatogr. A. 1217(2010) 5848-5858
4. J. Harynuk, T. Górecki, J. de Zeeuw, Overloading of the second-dimension column in comprehensive two-dimensional gas chromatography, J. Chromatogr. A. 1071 (2005) 21-27
5. Z. Zhu, J. Harynuk, T. Górecki, The Effect of the First-dimension Column Film Thickness on Comprehensive Two-dimensional Gas Chromatographic Separation, J. Chromatogr. A. 1105 (2006) 17-24
6. Z. Liu, J. B. Phillips, Comprehensive two-dimensional gas chromatography using an on-column thermal modulator interface, J. Chromatogr. Sci. 1067 (1991) 227-231
7. J. B. Phillips, C. J. Venkatramani, Comprehensive two-dimensional gas chromatography applied to the analysis of complex mixtures, J. Microcolumn Sep. 5 (1993) 511-516
8. P. Q. Tranchida, A. Casilli, P. Dugo, G. Dugo, L. Mondello, Generation of improved gas linear velocities in a comprehensive two-dimensional gas chromatography system, Anal. Chem. 79 (2007) 2266-2275
9. J. Harynuk, T. Gorecki, Comprehensive two-dimensional gas chromatography in stop-flow mode, J. Sep. Sci. 27 (2004) 431-441.
10. J. Harynuk, T. Gorecki, Comparison of comprehensive two-dimensional gas chromatography in conventional and stop-flow modes, J. Chromatogr. A 1105 (2006) 159-167.
11. N. Oldridge, O. Panic, T. Gorecki, Stop-flow comprehensive two-dimensional gas chromatography with pneumatic switching, J. Sep. Sci. 31 (2008) 3375-3384.
12. M. M. Koek, B. Muilwijk, L.L.P. van Stee, T. Hankemeier, Higher mass loadability in comprehensive two-dimensional gas chromatography-mass spectrometry for improved analytical performance in metabolomics analysis, J. Chromatogr. A. 1186 (2008) 420-429
13. C. Cordero, C. Bicchi, M. Galli, S. Galli, P. Rubiolo, Evaluation of different internal-diameter column combinations in comprehensive two-dimensional gas chromatography in flavour and fragrance analysis, J. Sep. Sci. 31 (2008) 3437-3450



14. D. Peroni, R.J. Vonk, W. van Egmond, H.-G. Janssen, Macroporous polymer monoliths as second dimension columns in comprehensive two-dimensional gas chromatography: a feasibility study, *J. Chromatogr. A* 1268 (2012) 139-149
15. D. Peroni, A.A.S. Sampat, W. van Egmond, S. de Koning, J. Cochran, R. Lautamo, H.-G. Janssen, Comprehensive two-dimensional gas chromatography with a multi-capillary second dimension: A new column-set format for simultaneous optimum linear velocity operation, *J. Chromatogr. A* 1317 (2013) 3-11
16. D. Peroni, H-G. Janssen, Comprehensive two-dimensional gas chromatography under high outlet pressure conditions: a new approach to correct the flow-mismatch issue in the two dimensions, *Journal of Chromatography A*, 1332 (2014) 57–63
17. P.Q. Tranchida, M. Zoccali, F.A. Franchina, A. Cotroneo, P. Dugo, L. Mondello, Gas velocity at the point of re-injection: an additional parameter in comprehensive two-dimensional gas chromatography optimization, *J. Chromatogr. A*. 1314 (2013) 216-223
18. R. Shellie, P. Marriott, P. Morrison, L. Mondello, Effects of pressure drop on absolute retention matching in comprehensive two-dimensional gas chromatography, *J. Sep. Sci.* 27 (2004) 504-512
19. European Directorate for the Quality of Medicines (EDQM). European Pharmacopoeia VIII ed. 2014
20. C. Bicchi, G. M. Nano, C. Frattini, On the composition of the essential oils of *Artemisia genepi* Weber and *Artemisia umbelliformis* Lam., *Z. Lebensm. Unters. Forsch.* 175 (1982) 182-185
21. J. Beens, H. G. Janssen, M. Adahchour, U. A. Th. Brinkman, Flow regime at ambient outlet pressure and its influence in comprehensive two-dimensional gas chromatography, *J. Chromatogr. A*. 1086 (2005) 141-150
22. C. Schutjes, P. Leclercq, J. Rijks, C. Cramers, C. Vidalmadjar, G. Guiochon, Model describing the role of the pressure gradient on efficiency and speed of analysis in capillary gas chromatography, *J. Chromatogr.* 289 (1984) 163-170
23. S.E. Reichenbach, X. Tian, C. Cordero, Q. Tao, Features for non-targeted cross-sample analysis with comprehensive two-dimensional chromatography, *J. Chromatogr. A* 1226 (2012) 140- 148
24. M. Mucciarelli, M. Maffei, Introduction to the genus. In *Medicinal and Aromatic Plants—Industrial Profiles: Artemisia*; Wright, C. W., Ed.; Taylor and Francis: London, U.K., 2002; pp 1– 50. Open URL UNIV STUDI DI TORINO
25. P. Rubiolo, M. Matteodo, C. Bicchi, G. Appendino, G. Gnani, C. Berteà, M. Maffei, Chemical and Biomolecular Characterization of *Artemisia umbelliformis* Lam., an Important Ingredient of the Alpine Liqueur “Genepi” *J. Agric. Food Chem.*, 57 (2009) 3436-3443
26. D. W. Lachenmeier, D. Nathan-Maister, T. A. Breaux, E. M. Sohnius, K. Schoeberl, T. Kuballa, Chemical composition of vintage preban absinthe with special reference to thujone, fenchone,

- pinocamphone, methanol, copper, and antimony concentrations, J. Agric. Food Chem. 56 (2008) 3073-3081
27. Council Directive (EC) No 1334/2008 on flavourings and certain food ingredients with flavouring properties for use in and on foods and amending Council Regulation (EEC) No 1601/91, Regulations (EC) No 2232/96 and (EC) No 110/2008 and Directive 2000/13/EC.
28. Robert P. Adams, Identification of Essential Oil Components by Gas Chromatography/Mass Spectrometry, 4th Edition, Allured books
29. P.Q. Tranchida, M. Zoccali, F.A. Franchina, P. Dugo, L. Mondello, Measurement of fundamental chromatography parameters in conventional and split-flow comprehensive two-dimensional gas chromatography-mass spectrometry: A focus on the importance of second-dimension injection efficiency, J Sep. Sci. 36 (2013) 212-218
30. IOFI. Analytical procedure for a general quantitative method using coupled capillary gas chromatography/mass spectrometry with selected ion monitoring (SIM). Z. Lebensm.-Unters.-Forsch. 1997, 204, 395.
31. ISO. Essential oils – Analysis by gas chromatography on capillary columns – General methods. International standard ISO 7609, International Organization for Standardization, Geneva, 1985
32. Recommended Practice Flavour Fragr. J. 26 (2011) 297
33. R. Costa, M.R. De Fina, M.R. Valentino, A. Rustaiyan, P. Dugo, G. Dugo, An investigation on the volatile composition of some *Artemisia* species from Iran, Flavour Fragr. J. 24 (2009) 75-82
34. C. Bicchi, E. Liberto, M. Matteodo, B. Sgorbini, L. Mondello, B. d'Acampora Zellner, Quantitative analysis of essential oils: a complex task, Flavour Fragr. J. 23 (2008) 382-391
35. R. Costa, B. d'Acampora Zellner, M. L. Crupi, M. R. De Fina, M. R. Valentino, P. Dugo, G. Dugo, L. Mondello, GC-MS, GC-O and enantio-GC investigation of the essential oil of *Tarhonanthus camphoratus* L., Flavour Fragr. J., 23 (2008) 40-48
36. J.Y. de Saint Laumer, E. Cicchetti, P. Merle, J. Egger, A. Chaintreau, Quantification in Gas Chromatography: Prediction of Flame Ionization Detector Response Factors from Combustion Enthalpies and Molecular Structures, Anal. Chem. 82 (2010) 6457-6462

508 **Caption to Figures**

509 **Figure 1:** 2D plots (upper part) and raw chromatograms of *n*-C13-*n*-C15 linear hydrocarbons, analyzed in  
510 isothermal conditions at 150°C, 296 kPa head-pressure and 5s of modulation period. **1a:** *Set-up I*; **1b:** *Set-up*  
511 *II* with the outlet pressure correction as indicated in the text.

512  
513 **Figure 2:** 2D plots of *Artemisia umbelliformis* essential oil, analyzed with *Set-up I* (**2a** full scan MS and **2b** FID  
514 signals), *Set-up II* (**2c** full scan MS and **2d** FID signals) and *Set-up III* (**2e** full scan MS and **2f** FID signals).  
515 Chemical classes: *m*: mono-terpene hydrocarbons, *s*: sesqui-terpenene hydrocabons, *mox*: oxygenated  
516 monoterpenoids, *sox*: oxygenated sesquiterpenoids, *mest*: mono terpenoid esters.

517  
518 **Figure 3:** <sup>2</sup>D retention time absolute differences (FID vs. MS) for: **3a:** *n*-alkanes from *n*-C9 to *n*-C25, **3b:**  
519 fourteen volatiles of interest for the flavor and fragrance field.

520  
521 **Figure 4:** <sup>1</sup>D (**4a**) and <sup>2</sup>D (**4b**) retention time variations for *Set-up I*, *Set-up II* (with and without outlet  
522 pressure correction) and *Set-up III*.

523  
524 **Figure 5:** 2D plots of *Artemisia umbelliformis* essential oil, the magnified region corresponds to the elution  
525 area of 2-methylbutyl isovalerate, nonanal and α-thujone. **5a:** the separation pattern obtained from *Set-up*  
526 *II*, and the corresponding raw chromatogram, **5b:** *Set-up III* separation. Apparent resolution values are  
527 reported in the text.

528

529 **Caption to Tables**

530 **Table 1:** Column configurations, column head pressure ( $p_i$ ) and midpoint pressure (i.e., estimated pressure  
531 at the junction between the 1D column and the two secondary columns -  $p_2$ ), estimated linear velocities in  
532 the  $^1D$  and two  $^2Ds$  ( $^1\bar{u}$ ,  $^2\bar{u}_{MS}$ ,  $^2\bar{u}_{FID}$ ), hold-up times and calculated split-ratio.

533  
534 **Table 2:**  $^1D$  (min) and  $^2D$  (sec) retention times,  $^2D$  absolute errors (sec), half-height peak-width (ms),  
535 number of scans/points per (modulated) peak, normalized 2D Volumes (normalization on geranyl acetate)  
536 obtained by analyzing the FFStd2 model mixture with *Set-up II* and *Set-up III*.

537  
538 **Table 3:** *Artemisia umbelliformis* essential oil target analytes listed, together with experimental and  
539 tabulated [28] Linear Retention Indices in the  $^1D$  ( $I_s^T$ ), MS match factors resulting from the NIST Identity  
540 Spectrum Search algorithm, Signal-to-Noise values (Peak-to-Peak S/N as calculated by the Agilent algorithm  
541 - SNR) estimated on the highest modulation of each 2D peak, Normalized 2D Volumes (normalization was  
542 done on the Internal Standard n-C12) for *Set-ups II* and *III*.

543

Table 1

<sup>1</sup> D column		<sup>2</sup> D column(s)	Carrier gas (He) <sup>a</sup>	
			Auxiliary EPC correction	
<b>Set-up I</b>	30 m, 0.25 mm d <sub>c</sub> , 0.25 µm d <sub>f</sub> SE52 (95% polydimethylsiloxane, 5% phenyl) Mega (Legnano, Milan, Italy)	to MS detector: 1.6 m - to FID detector: 1.4 m column dimensions: 0.1 mm d <sub>c</sub> , 0.10 µm d <sub>f</sub> OV1701 (86% polydimethylsiloxane, 7% phenyl, 7% cyanopropyl) Mega (Legnano, Milan, Italy)	$p_1$ : 296.0 KPa $p_2$ : 182.6 KPa $^1\bar{u}$ : 34.3 cm/s $^2\bar{u}_{MS}$ : 195 - hold-up: 0.8 s $^2\bar{u}_{FID}$ : 178 - hold-up: 0.8 s split ratio (MS/FID): 50:50	
<b>Set-up II</b>	30 m, 0.25 mm d <sub>c</sub> , 0.25 µm d <sub>f</sub> SE52 (95% polydimethylsiloxane, 5% phenyl) Mega (Legnano, Milan, Italy)	to MS detector: 1.4 m - to FID detector: 1.4 m column dimensions: 0.1 mm d <sub>c</sub> , 0.10 µm d <sub>f</sub> OV1701 (86% polydimethylsiloxane, 7% phenyl, 7% cyanopropyl) deactivated capillary to MS detector: 0.17 m, 0.1 mm d <sub>c</sub> Mega (Legnano, Milan, Italy)	$p_1$ : 296.0 KPa $p_2$ : 181.9 KPa $p_{aux}$ : Off $^1\bar{u}$ : 34.5 cm/s $^2\bar{u}_{MS}$ : 198 - hold-up: 0.8 s $^2\bar{u}_{FID}$ : 177 - hold-up: 0.8 s split ratio (MS/FID): 51:49	$p_1$ : 296.0 KPa $p_2$ : 182.6 KPa $p_{aux}$ : 39.9 KPa (relative) $^1\bar{u}$ : 34.2 cm/s $^2\bar{u}_{MS}$ : 180 - hold-up: 0.8 s $^2\bar{u}_{FID}$ : 180 - hold-up: 0.8 s split ratio (MS/FID): 50:50
<b>Set-up III</b>	30 m, 0.25 mm d <sub>c</sub> , 0.25 µm d <sub>f</sub> SE52 (95% polydimethylsiloxane, 5% phenyl) Mega (Legnano, Milan, Italy)	column dimensions: 1.4 m, 0.1 mm d <sub>c</sub> , 0.10 µm d <sub>f</sub> OV1701 (86% polydimethylsiloxane, 7% phenyl, 7% cyanopropyl) deactivated capillaries for effluent splitting to parallel detectors: to MS detector: 0.4 m, 0.1 mm d <sub>c</sub> - to FID detector: 0.25 m, 0.1 mm d <sub>c</sub> Mega (Legnano, Milan, Italy)	$p_1$ : 280.0 KPa $p_2$ : 205.1 KPa $^1\bar{u}$ : 22.8 cm/s $^2\bar{u}$ : 240 - hold-up: 0.6 s split ratio (MS/FID): 50:50	
<sup>a</sup> : reported values were calculated on the basis of reference equations and are just approximations of real ones				

Table 2

Compound Name	Set-up II									Set-up III							
	MS (TIC signal)						FID signal			MS (TIC signal)					FID signal		
	<sup>1</sup> D (min)	<sup>2</sup> D (sec)	<sup>2</sup> D Error (sec)	Half height pw (ms)	Number of scans	Norm 2D Volume	Half height pw (ms)	Points per peak	Norm 2D Volume	<sup>1</sup> D (min)	<sup>2</sup> D (sec)	Half height pw (ms)	Number of scans	Norm 2D Volume	Half height pw (ms)	Points per peak	Norm 2D Volume
α-Pinene	8.25	1.58	0.04	60	21	1.468	60	144	1.358	11.92	1.27	60	14	1.36	60	79	1.153
Benzaldehyde	9.34	2.61	0.02	120	19	0.757	60	89	0.898	13.17	2.02	120	15	0.462	60	115	0.563
Benzyl Alcohol	12.34	3.71	-0.02	180	27	0.424	120	162	0.860	16.42	2.78	180	23	0.428	120	158	0.726
α-Thujone	15.42	2.68	0.00	120	27	0.993	60	113	1.002	19.84	2.02	120	21	0.871	120	86	0.903
Camphor	17.25	2.86	-0.01	120	20	1.400	120	162	1.280	21.84	2.10	120	16	1.160	120	99	1.152
Carvone	21.75	3.05	-0.02	120	23	0.543	120	207	0.801	26.34	2.26	120	19	0.535	120	115	0.707
Cinnamyl Alcohol	24.84	4.10	-0.20	180	27	0.070	120	297	0.473	29.17	2.86	180	26	0.057	120	252	0.379
Geranyl acetate	27.67	2.57	-0.04	120	30	1.000	60	126	1.000	32.17	1.90	120	29	1.000	60	86	1.000
Vanillin	28.50	4.81	-0.13	180	25	0.155	180	207	0.831	33.09	3.45	240	31	0.126	180	209	0.551
Coumarin	30.09	4.62	-0.18	180	33	0.241	120	144	0.823	34.92	3.33	240	29	0.187	120	187	0.541
Isoeugenol	30.59	3.57	-0.12	120	23	0.372	120	279	0.809	35.25	2.54	180	36	0.256	120	125	0.716
Isoeugenyl acetate	36.92	3.71	-0.11	120	21	0.481	120	225	0.693	41.5	2.66	120	21	0.438	120	101	0.791
Benzyl Benzoate	42.75	3.12	0.02	120	56	0.475	120	234	0.710	47.59	2.42	180	29	0.425	120	259	0.799
Sclareol	57.09	3.40	-0.01	180	41	0.828	120	153	1.273	61.92	2.62	240	31	0.530	120	145	1.179

Table 3

#ID	Compound Name	Exp. $I_s^T$	Ref. $I_s^T$ <sup>a</sup>	Set-up II		Set-up III		Set-up II	Set-up III	Set-up II	Set-up III
				MS Match Factor	SNR	MS Match Factor	SNR	Norm 2D Volume MS (TIC) signal		Norm 2D Volume FID signal	
1	Thujene	918	931	884	3740	906	3433	0.452	0.552	0.242	0.249
2	$\alpha$ -Pinene	925	939	860	12791	833	12232	0.542	0.746	0.666	0.679
3	Camphene	941	953	909	4170	913	3828	0.910	0.978	0.356	0.367
4	Sabinene	966	976	874	63223	893	53153	5.757	5.830	3.477	3.548
5	$\beta$ -Pinene	970	980	892	44034	889	40563	9.521	9.150	4.063	4.190
6	$\beta$ -Myrcene	984	991	905	10080	901	9252	2.023	2.185	0.802	0.825
7	p-Cymene	1021	1026	917	59306	915	49859	12.652	15.281	6.166	6.358
8	Limonene	1025	1031	913	3965	927	3640	0.472	0.509	0.271	0.280
9	1,8-Cineole	1029	1033	907	88187	892	84336	47.829	51.810	19.558	20.169
10	$\gamma$ -Terpinene	1056	1062	853	17482	875	16046	1.900	2.856	1.513	2.259
11	cis-Sabinenehydrate	1067	1068	883	9225	869	7755	2.282	3.878	1.654	1.706
12	$\alpha$ -Terpinolene	1085	1088	865	4416	870	4054	0.750	0.861	0.475	0.489
13	2-Methylbutyl isovalerate	1111	1109	912	1264	-	-	0.001	-	0.367	-
14	$\alpha$ -Thujone	1111	1102	903	63176	890	57988	452.460	482.096	157.457	160.677
15	Nonanal	1113	1098	881	1409	-	-	0.193	-	0.000	-
16	$\beta$ -Thujone	1120	1114	895	57087	896	52588	135.454	148.909	48.767	49.765
17	trans-Pinocarveol	1143	1139	887	4458	-	-	1.841	-	2.263	-
18	Borneol	1174	1165	891	33002	892	30292	42.580	45.591	14.182	14.625
19	4-Terpineol	1183	1177	900	44096	886	37072	57.102	58.992	15.904	16.400
20	$\alpha$ -Terpineol	1198	1189	913	16567	902	15261	15.234	17.996	4.641	4.736
21	Myrtanal	1198	1193	903	13368	874	12271	21.345	18.852	7.579	7.815
22	7-Methyl-3-octen-2-one	1204	-	843	1165	803	1114	1.248	1.279	0.394	0.403
23	cis-Piperitol	1213	1193	859	2035	882	1868	1.134	1.256	0.668	0.689
24	Nerol	1228	1228	807	1355	844	1139	1.826	2.240	0.602	0.619
25	Cuminic aldehyde	1244	1239	861	3089	860	2836	2.294	2.263	1.025	1.057
26	Bornyl acetate	1287	1285	910	8634	918 <sup>b</sup>	8257	6.243	6.450	1.414	1.458
27	Sabinyl acetate	1293	1291	939	4675	864 <sup>b</sup>	4291	1.281	-	1.186	-
28	$\alpha$ -Terpinil acetate	1350	1350	876	29759	879	25019	14.014	15.140	5.269	7.870
29	$\alpha$ -Copaene	1381	1376	896	7647	909	7044	3.616	3.343	1.376	1.419
30	Unknown	1381	-	-	31021	-	28474	15.042	18.534	5.693	5.869
31	Sabinyl isobutyrate	1416	1416	890 <sup>c</sup>	65107	912 <sup>c</sup>	59761	76.197	71.710	21.347	22.014
32	$\beta$ -caryophyllene	1425	1418	906	42265	908	40419	23.470	23.208	6.945	7.087
33	trans- $\beta$ -farnesene	1459	1458	871	35327	876	32425	21.491	23.573	6.891	7.106
34	Unknown	1469	-	-	10659	-	9784	5.545	5.772	1.853	1.891
35	Germacrene D	1488	1480	900	21754	881	20804	14.768	14.192	5.276	5.441
36	Biciclogermacrene	1502	1494	869	10547	-	-	7.875	-	1.786	-
37	Sabinyl isovalerianate	1506	1503	906 <sup>c</sup>	71628	905 <sup>c</sup>	60219	76.137	86.920	39.133	40.355
38	$\beta$ -bisabolene	1515	1509	890	3808	782	3508	1.745	1.389	0.439	0.453
39	Sabinyl valerianate	1519	1516	892 <sup>c</sup>	62671	896 <sup>c</sup>	57524	93.136	95.015	27.224	28.074
40	$\delta$ -cadinene	1526	1524	846	9409	858	8998	5.033	4.948	1.698	2.536
41	$\gamma$ -undecalactone	1579	1606	867	1963	902	1802	1.208	1.296	0.560	0.578
42	Spathulenol	1585	1576	874	46948	805 <sup>b</sup>	39470	57.990	-	15.830	-

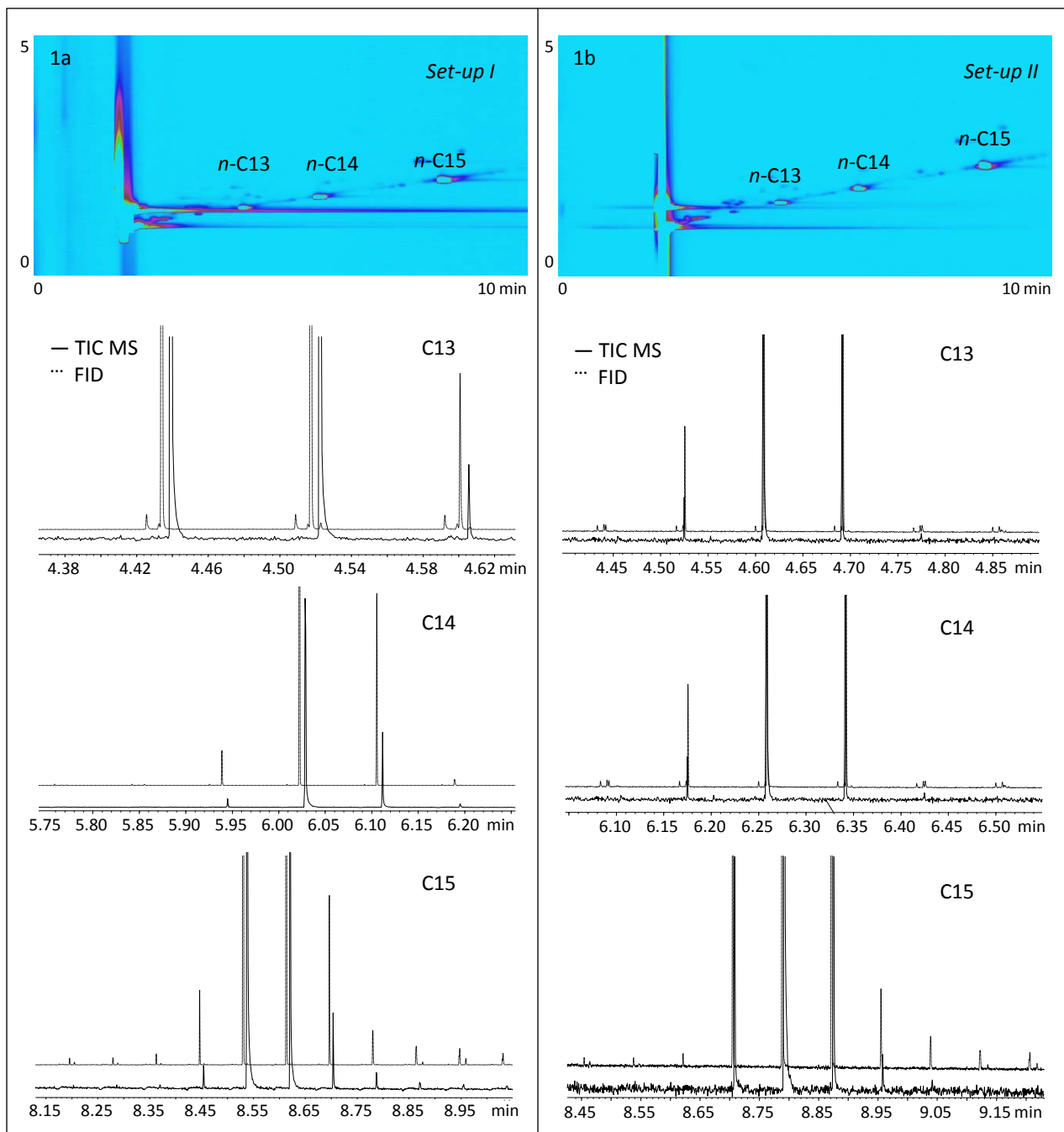
43	Neryl isovalerianate	1587	1584	817 <sup>c</sup>	60494	896 <sup>c</sup>	55527	1.942	112.811	31.251	32.226
44	Caryophyllene oxide	1589	1581	905	28691	890 <sup>b</sup>	27437	31.000	84.891	11.036	28.262
45	Unknown	1632	-	-	36098	-	33133	0.098	0.137	15.677	16.167
46	Unknown	1675	-	-	14160	-	11905	25.263	23.381	4.651	4.785
47	γ-dodecalactone	1686	1671	817	1038	854	956	1.294	1.657	0.429	0.442
48	Unknown	1895	-	-	4419	-	4056	3.395	3.374	1.515	1.562
49	Unknown	1918	-	-	14011	-	12861	13.989	14.268	4.327	4.462
50	Unknown MW 232	1951	-	-	10077	-	9637	11.791	12.280	4.034	4.632
51	Unknown	2056	-	-	12421	-	11401	10.115	10.479	3.026	3.120

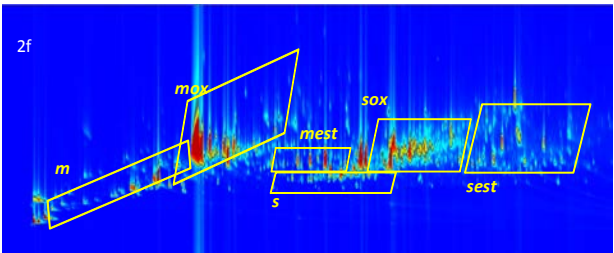
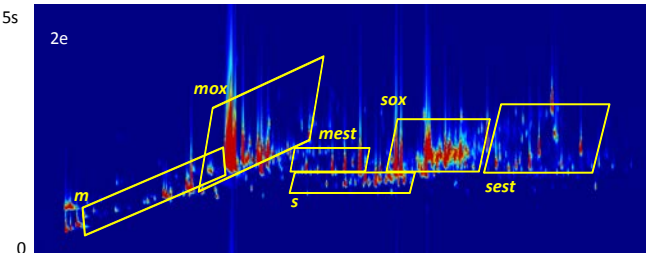
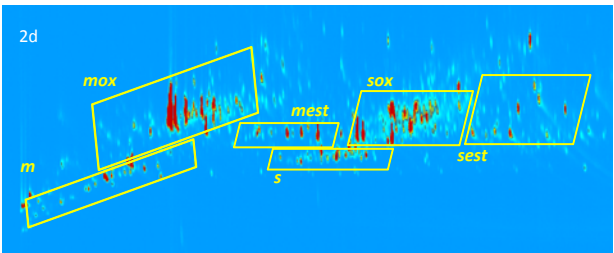
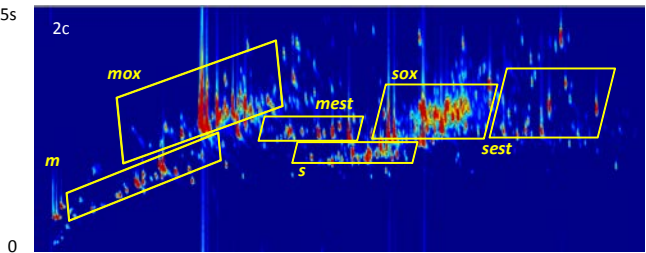
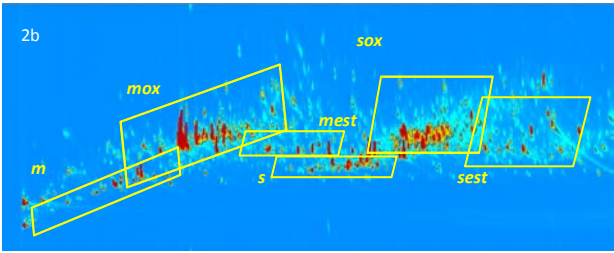
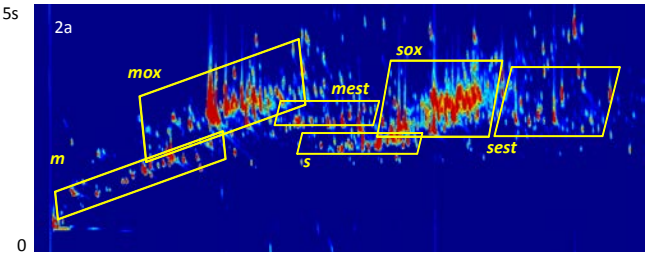
<sup>a</sup>: Adams Essential Oils database Ref. 28

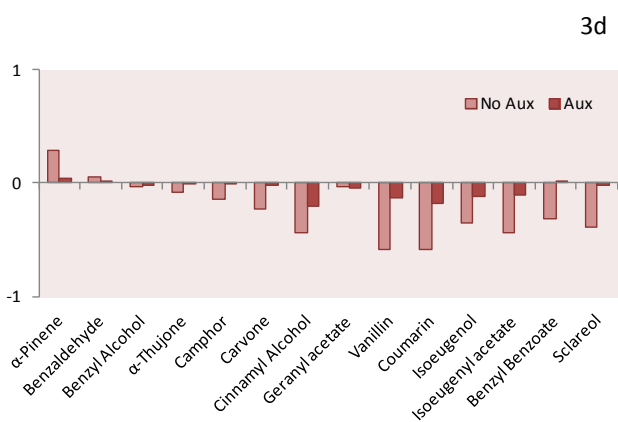
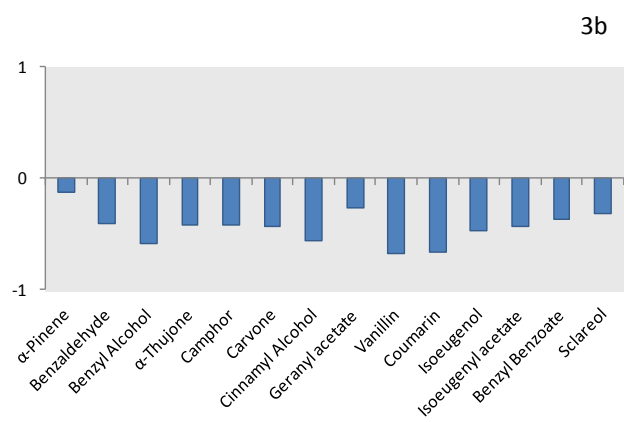
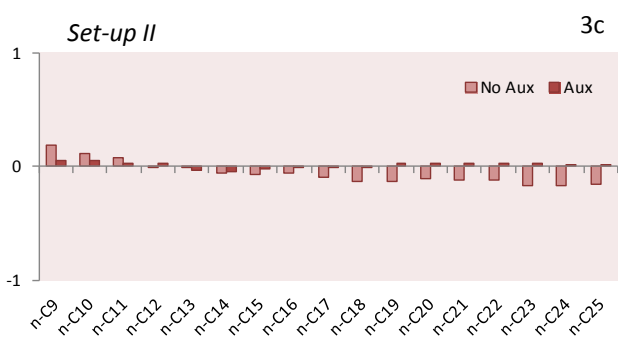
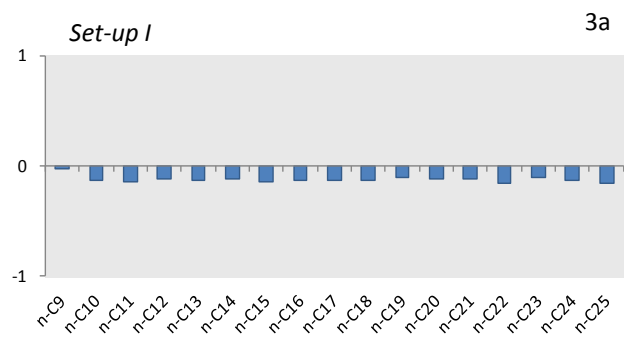
<sup>b</sup>: partial coelution

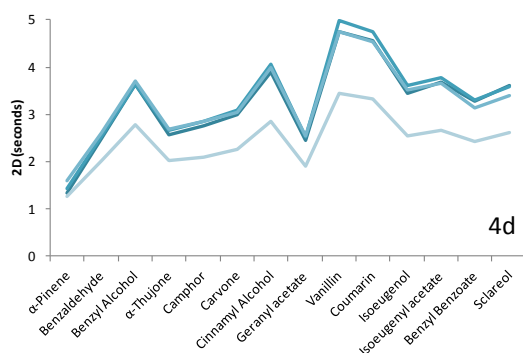
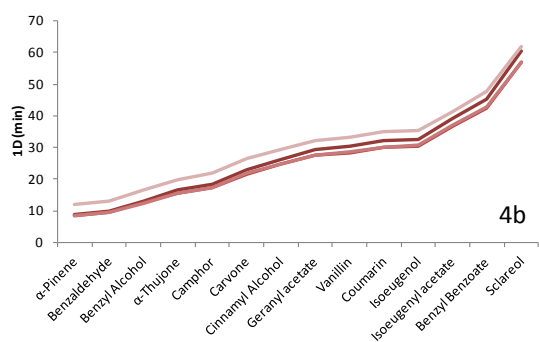
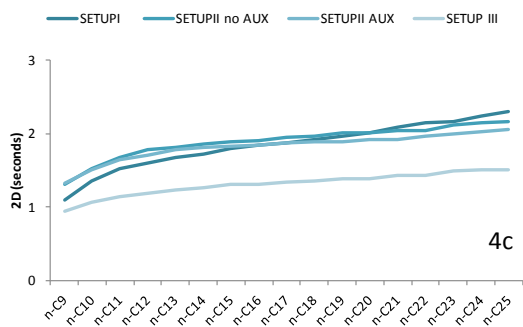
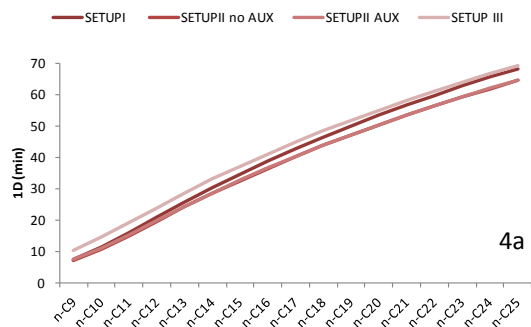
<sup>c</sup>: authentic standards ad-hoc synthesized Ref. 25

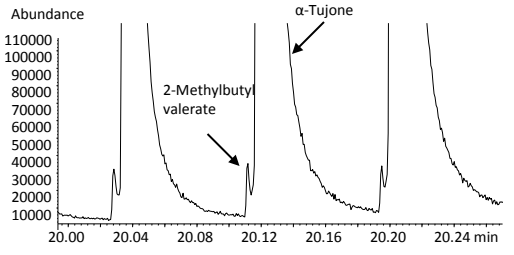
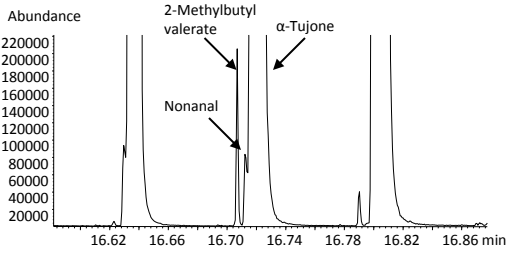
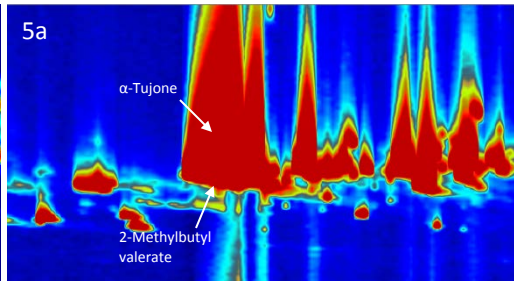
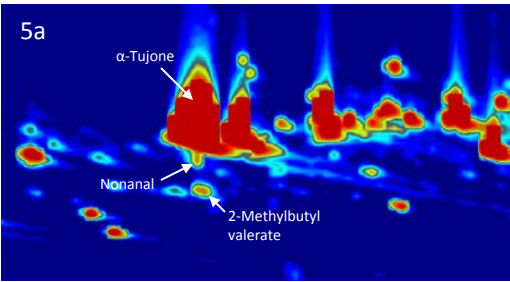




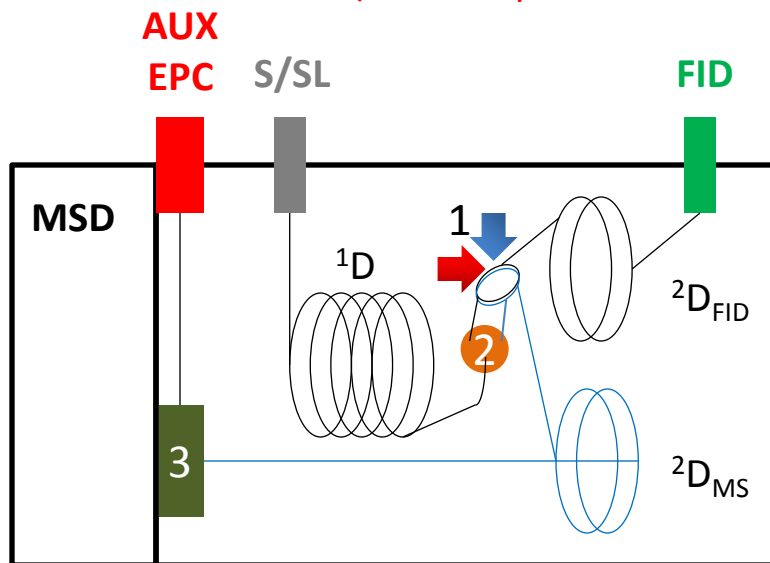








1. Loop-Type thermal modulator  
(Zoex Corporation, Houston, TX)



2. Microfluidic 3-port splitter  
(Sil-flow™- SGE Ringwood,  
Victoria, Australia)

3. Outlet pressure compensation  
Microfluidic device (Quick-Swap™- Agilent)